

000
001
002
003
004
005
006
007
008
009
010
011
012
013
014
015
016
017
018
019
020
021
022
023
024
025
026
027
028
029
030
031
032
033
034
035
036
037
038
039
040
041
042
043
044
045
046
047
048
049
050
051
052
053

THE COOPER UNION
ALBERT NERKEN SCHOOL OF ENGINEERING

A Partitioned Autoencoder
for Audio De-Noising

by
Ethan Lusterman

A thesis submitted in partial fulfillment
of the requirements for the degree of
Master of Engineering

September 2016

Professor Sam Keene, Advisor

054 THE COOPER UNION FOR THE
055
056 ADVANCEMENT OF SCIENCE AND ART
057
058
059
060

061 ALBERT NERKEN SCHOOL OF ENGINEERING
062
063
064
065
066
067
068
069

070 This thesis was prepared under the direction of the Can-
071 didate's Thesis Advisor and has received approval. It was
072 submitted to the Dean of the School of Engineering and
073 the full Faculty, and was approved as partial fulfillment of
074 the requirements for the degree of Master of Engineering.
075
076
077
078
079
080
081
082
083
084
085
086

087 _____
088 Dean, School of Engineering Date
089
090
091
092
093
094

095 _____
096 Prof. Sam Keene, Thesis Advisor Date
097
098
099
100
101
102
103
104
105
106
107

Acknowledgements

This thesis would not be possible without the guidance and support from my advisor, Dr. Sam Keene. He has mentored me since I was an undergraduate, and I am grateful for him helping this project come to life. I also want to thank Christopher Curro, my informal second advisor who helped me to think outside the box and for whom the overall system architecture is named after.

I would like to thank Kate Thorsen for pushing me past my potential and encouraging me to stay positive despite the frustrations of research. Lastly, I would like to thank my friends and family for their support. This thesis would not have been possible without all their support.

Abstract

Traditional audio denoising systems are often linear time-invariant (LTI) and often require access to clean data to properly train to remove noise. Since clean audio is often unavailable, we build on a partitioned denoising autoencoder for denoising audio signals when clean examples are unavailable for training. In addition, the nonlinearity of a neural network architecture provides additional gains over standard linear models. We compare existing semi-supervised denoising systems as well as canonical supervised denoising autoencoders. We show that for moderate levels of noise, our autoencoder can outperform existing schemes.

216
217
218
219
220
221
222
223
224
225
226
227
228
229
230
231
232
233
234
235
236
237
238
239
240
241
242
243
244
245
246
247
248
249
250
251
252
253
254
255
256
257
258
259
260
261
262
263
264
265
266
267
268
269

Contents

1	Introduction	1
2	Background	3
2.1	Machine Learning	3
2.1.1	Regression	4
2.1.2	Overfitting and Curse of Dimensionality	4
2.1.3	Loss functions and Regularization	4
2.1.4	Gradient Stuff?	4
2.2	Neural Networks	4
2.2.1	Dense Layer	6
2.2.2	Denoising Autoencoder	6
2.2.3	Convolutional Layer	7
2.2.4	Network Training	7
2.2.5	Regularization	7
2.2.6	Choice of Activation Function	7
2.2.7	Minibatch Training	9
2.2.8	Batch Normalization	10
2.3	Signals and Systems	10
2.3.1	Signals	10
2.3.2	Convolution	11
2.3.3	Frequency Transforms	12
2.3.4	Windowing and Perfect Reconstruction	13
2.3.5	Window Size and Frequency v. Time Resolution Tradeoff	14
2.3.6	Noise and Signal-to-Noise Ratio	14
2.3.7	Magnitude and Phase Spectrum	14
3	Signal Model and Data	15
3.1	Network Input and Output	15
3.2	Signal and Noise Choices	17
3.3	Other Network Parameters	17

270	4 De-noising Architectures	19
271		
272	4.1 Supervised Autoencoder	19
273		
274	4.2 Partitioned Autoencoder	21
275	4.2.1 Phase Reconstruction	23
276		
277	4.3 Curro Autoencoder	24
278		
279		
280	5 Results	26
281		
282	5.1 Supervised Autoencoder	26
283	5.1.1 Batch Normalized Input	26
284	5.1.2 Non-Batch Normalized Input	26
285		
286	5.2 Partitioned Autoencoder	26
287		
288	5.3 Partitioned Curro Autoencoder	26
289		
290	5.4 Comparison of Loss Convergence	26
291		
292	5.5 Comparison of Mean Squared Error Convergence	26
293		
294	6 Conclusions and Future Work	27
295		
296	6.1 Conclusions	27
297		
298	6.2 Future Work	28
299	6.2.1 Models	28
300	6.2.2 Data	29
301		
302		
303		
304		
305		
306		
307		
308		
309		
310		
311		
312		
313		
314		
315		
316		
317		
318		
319		
320		
321		
322		
323		

324
325
326
327
328
329
330
331
332
333
334
335
336
337
338
339
340
341
342
343
344
345
346
347
348
349
350
351
352
353
354
355
356
357
358
359
360
361
362
363
364
365
366
367
368
369
370
371
372
373
374
375
376
377

List of Figures

1	Example neural network	5
2	Modified Rectified Linear Unit Activation	20
3	Example Partitioned Masking Matrix	22
4	Loss at various SNRs for Supervised Single-Layer Autoencoder with Batch Normalization at the Input	26
5	MSE at various SNRs for Supervised Single-Layer Autoencoder with Batch Normalization at the Input	27
6	Loss at various SNRs for Supervised Single-Layer Autoencoder without Batch Normalization at the Input	27
7	MSE at various SNRs for Supervised Single-Layer Autoencoder with Batch Normalization at the Input	28
8	Loss at various SNRs for Single-Layer Partitioned Autoencoder [1]	28
9	MSE at various SNRs for Single-Layer Partitioned Autoencoder [1]	29
10	Loss at various SNRs for Single-Layer Curro Autoencoder . .	29
11	MSE at various SNRs for Single-Layer Curro Autoencoder . .	30
12	Loss Comparison of Various Networks at -6 dB	30
13	Loss Comparison of Various Networks at -3 dB	31
14	Loss Comparison of Various Networks at 0 dB	31
15	Loss Comparison of Various Networks at 3 dB	32
16	Loss Comparison of Various Networks at 6 dB	32
17	MSE Comparison of Networks at -6 dB	33
18	MSE Comparison of Networks at -3 dB	33
19	MSE Comparison of Networks at 0 dB	34
20	MSE Comparison of Networks at 3 dB	34
21	MSE Comparison of Networks at 6 dB	35

378	Table of Nomenclature
379	
380	
381	
382	
383	
384	
385	
386	
387	
388	
389	
390	
391	
392	
393	
394	
395	
396	
397	
398	
399	
400	
401	
402	
403	
404	
405	
406	
407	
408	
409	
410	
411	
412	
413	
414	
415	
416	
417	
418	
419	
420	
421	
422	
423	
424	
425	
426	
427	
428	
429	
430	
431	

1 Introduction

Advances in smartphone technology have led to smaller devices with more powerful audio hardware, allowing for common consumers to make higher quality recordings. However, recorded speech and music are subject to noisy conditions, often hampering intelligibility and listenability. The goal of denoising audio recordings is to improve intelligibility and perceived quality. A variety of applications of audio denoising exist, including listening to a recording of a band or an artist’s live performance in a noisy crowd, or listening to a recorded conversation or speech under noisy conditions.

A common technique for denoising involves the use of autoencoder neural networks. [2] Advances in parallel graphics processing units (GPU) and in machine learning algorithms have allowed for training deeper networks faster, utilizing more hidden layers with more neurons.

Prior work in denoising audio has involved the use of noise-free training data. Since common consumers do not often have access to clean audio, we seek to denoise without the use of clean audio. Other work has touched on such a semi-supervised scenario but was used more as a preprocessing step to a classification algorithm than as time-domain denoising. [1]

In this thesis, we compare several neural network architectures and problem scenarios, ranging from data input types, level of noise, depth of network, training objectives, and more. In Chapter 2, we present background information on machine learning, neural networks, and signal processing as well as prior work in audio denoising. In Chapter 3, we detail the problem formally as well as introduce our signal model and sourced data. In Chapter 4, we detail all considered network architectures. In Chapter 5, we compare results

486 from different data inputs, levels of noise, network architectures, and training
487
488 objectives and discuss methods of evaluation. Finally, we make conclusions
489
490 and recommendations for future work in Chapter 6.
491

2 Background

2.1 Machine Learning

Machine learning involves the use of computer algorithms to make decisions based on training data. Generally, this falls into categorizing input data (classification) or determining a mathematical function to determine a continuous output given an input (regression). Popular classification examples include recognizing handwritten digits (MNIST) as well as determining whether an image contains a cat or a dog. (REF) An example of a regression problem is determining the temperature given a set of input features (humidity, latitude, longitude, date, etc.).

Problems where training data contain input data vectors as well as the correct output vectors (targets) are known as supervised learning problems. Training a model to denoise audio where noise was introduced to the clean audio would be a supervised learning problem. On the other hand, training a model to denoise audio where the underlying clean signal is not known is an unsupervised learning problem. Different loss (objective) functions and neural network architectures can be exploited to accomplish denoising without the clean data.

For the purposes of this thesis, we use machine learning to determine an underlying nonlinear function that removes noise from time slices of audio (i.e. regression). These slices can then be pieced back together through overlap-add resynthesis. To clarify, this is a general linear model that maps an input noisy audio vector $y[n] = x[n] + N[n]$ to $\tilde{x}[n]$, a target denoised audio vector, where $x[n]$ is the underlying clean signal and $N[n]$ is the additive background noise.

2.1.1 Regression

A classical regression technique is linear regression, where one or more independent variables x_i are used to determine a scalar dependent variable y . The case of a single independent variable x is known as simple linear regression. More formally, for k independent variables, we would like to determine a weight vector \mathbf{w} and bias vector \mathbf{b} :

$$y_i = w_1 x_{i1} + \dots + w_k x_{ik} + b_i, \quad i = 1 \dots, n \quad (1)$$

$$\mathbf{y} = \mathbf{x}^T \mathbf{w} + \mathbf{b} \quad (2)$$

where the rows of \mathbf{x}^T are the example input observations and \mathbf{y} and \mathbf{b} are column vectors.

By extension, the case of linearly estimating a vector output giving a vector input is known as a generalized linear model. A canonical example would be estimating a sine wave $x[n]$ over some number of N samples given noisy samples $y[n] = x[n] + N[n]$.

2.1.2 Overfitting and Curse of Dimensionality

2.1.3 Loss functions and Regularization

2.1.4 Gradient Stuff?

2.2 Neural Networks

In this thesis, we deal only with feed-forward neural networks, which are essentially directed acyclic graphs (DAG) for computation. In other words, information only moves through the network in one direction. An example neural network is shown in Figure 1.

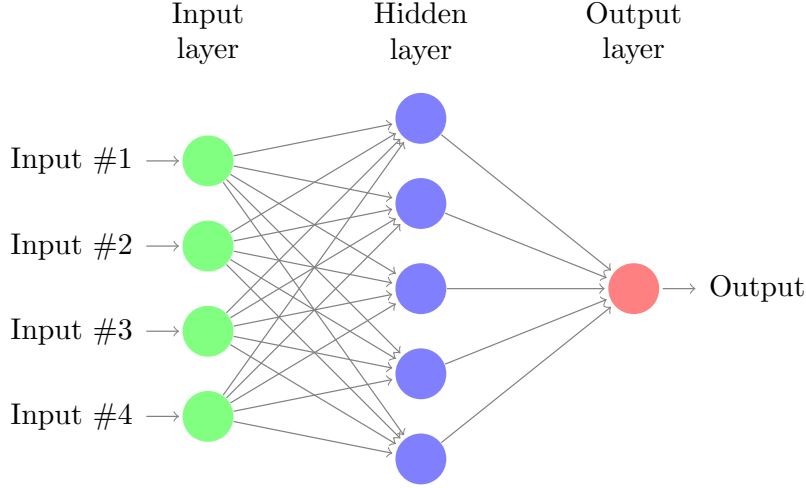


Figure 1: An example neural network. There are 4 input variables, 1 hidden layer with 5 neurons, and 1 output variable.

The connections in a neural network can be represented by linear combinations of the input variables with learned weights \mathbf{w} . [3] Unlike standard linear models however, neural networks apply a nonlinear activation $f(\cdot)$ at the output of each neuron. The circle nodes in a neural network diagram can be thought of as the sum of the linear combinations of the connection edges and the application of the bias and activation function. Therefore, a hidden neuron z_j in a network with N input variable nodes, M hidden nodes, and K output nodes takes on the value

$$z_j = f(a_j) \quad (3)$$

where the activation a_j is given by

$$a_j = \sum_{i=1}^N w_{ji}^{(1)} x_i + w_{j0}^{(1)} \quad (4)$$

The connection values w_{ji} are referred to as weights, and the scalars w_{j0} are referred to as biases. Note that the superscripted numbers refer to the Then, the output y_k is given by

$$y_k = g(a_k) \quad (5)$$

where the output activation a_k is given by

$$a_k = \sum_{j=1}^M w_{kj}^{(2)} z_j + w_{k0}^{(2)} \quad (6)$$

We are free to choose activation functions, which we will discuss later. However, note that at the output, the function $g(\cdot)$ is often an identity for regression problems and a sigmoid $\sigma(\cdot)$ for classification problems.

Often, the weights and biases are grouped into a weight vector \mathbf{w} . In other words, similar to the linear models described earlier, a neural network is a nonlinear function of input variables $\{x_i\}$ to output variables $\{y_k\}$ where the parameters of the function are learned via training techniques.

2.2.1 Dense Layer

Described in the previous section, we refer to a dense layer as a fully connected neural network, in which no interconnections between neurons are missing at each layer. Dense layers can be prone to overfitting. However, as we mention later, overfitting is not an immediate concern for the purposes of this thesis.

2.2.2 Denoising Autoencoder

An autoencoder is normally an abstraction of neural networks in which an encode function $\mathbf{Z} = f(\mathbf{X})$ and a decode function $\hat{\mathbf{X}} = g(\mathbf{Z})$ are learned to

learn a lower-dimensional representation of some input \mathbf{X} . [1] A denoising autoencoder is a supervised process whereby the clean input is first corrupted by some stochastic process $\mathbf{Y} = u(\mathbf{X})$. In other words, the neural network input would be a noisy input Y , and the network would try to learn weights such that the network output $\hat{\mathbf{X}}$ approximates the clean input \mathbf{X} . Another way to frame it is that your network is learning the inverse function of the noise process $u(\mathbf{x})$.

2.2.3 Convolutional Layer

2.2.4 Network Training

In order to train a neural network, we must update the weights such that we minimize a loss function, often some kind of sum-of-square error function. [3]

2.2.5 Regularization

2.2.6 Choice of Activation Function

The most common activation functions used are the logistic sigmoid function and the hyperbolic tangent. [2] The logistic sigmoid function is given by

$$g(x) = \frac{1}{1 + \exp(-x)} \quad (7)$$

Note that the sigmoid function has an output on the range $(0, 1)$. The hyperbolic tangent function (\tanh) is given by

$$g(x) = \frac{\sinh x}{\cosh x} \quad (8)$$

$$= \frac{\exp(x) - \exp(-x)}{\exp(x) + \exp(-x)} \quad (9)$$

$$= \frac{1 - \exp(-2x)}{1 + \exp(-2x)} \quad (10)$$

Note that the hyperbolic tangent function has an output on the range $(-1, 1)$.

Generally, our choice of nonlinearity should be chosen such that the expected range of desired output matches the nonlinearity's. In the case of audio denoising, different activations can be chosen depending on the input format. For example, time-domain audio frames are often processed with a digital floating point representation on the range of $[-1, 1]$. In such a case, the hyperbolic tangent might be appropriate. On the other hand, if we were working with magnitude spectra of an audio signal, we would use a linearity with an output range of $[0, \infty]$.

Recently, a more popular activation function which has in use is the rectified linear unit (ReLU). [4] The ReLU is defined by the following:

$$g(x) = \begin{cases} 0 & \text{if } x < 0 \\ x & \text{if } x \geq 0 \end{cases} \quad (11)$$

In other words, $g(x) = \max(0, x)$. This function satisfies the range of output we expect for magnitude spectra. In terms of gradient calculations, the zero derivative for negative input values of x can cause nodes to not be activated, potentially leading to gaps in information at the output and slower training time. To combat this, variations of the ReLU are used which have small, non-zero gradients for negative input values. For example, leaky ReLU's are defined by

$$g(x) = \begin{cases} 0.01x & \text{if } x < 0 \\ x & \text{if } x \geq 0 \end{cases} \quad (12)$$

Advantages of ReLU's include better gradient propagation as well as fast computation and sparse representation. Some disadvantages include non-differentiability at $x = 0$. Also, depending on use case, sparse representation might not be desired.

2.2.7 Minibatch Training

Historically, neural networks were trained one example at a time (online) or in a batch (all examples at once). [5] For the online approach, the network weights are updated after gradients are calculated and backpropagated for each training example. On the other hand, the batch approach accumulates average gradients for all examples and then updates the network weights. The batch approach might approximate the true gradients better than the online approach, but the online approach tends to have faster training time and convergence. [5] This is because with an online approach, the network is less likely to get stuck in a local minimum.

Minibatch training has become more popular recently. Serving as a midway point between the two approaches, minibatch training exposes the network to a small number of examples and then accumulates gradients and updates the network weights. The trend toward minibatch training comes at a time where parallel computing resources are easily accessible.

2.2.8 Batch Normalization

Batch normalization is a technique that helps to speed up training time and convergence. Batch normalization accumulates learned statistics of the network to help achieve loss convergence more quickly. More formally,

2.3 Signals and Systems

Domain knowledge of discrete audio signals and systems better informs our decisions for an audio denoising system, so some background information on signals and systems as it pertains to this thesis is detailed below.

2.3.1 Signals

We deal exclusively with discrete-time audio signals in this thesis. A discrete-time audio signal $x[n]$ is represented as a sequence of numbers (samples), where each integer-valued slot n in the sequence corresponds to a unit of time based on the sampling frequency f_s . This comes from sampling the continuous-time audio signal $x_c(t)$:

$$x[n] = x_c(nT) \quad (13)$$

where $T = 1/f_s$. For example, a 1-second speech signal sampled at 8kHz has 8000 samples. Furthermore, digital signals also have discrete valued sample amplitudes. For the purposes of this thesis, the bit depths of computers we use for analysis are high enough to allow for perfect reconstruction between continuous-time signals and digital signals.

We also assume signals collected have been properly sampled according to the Nyquist-Shannon sampling theorem, which states that a discrete-time signal

must be sampled at at least twice the highest frequency present in the signal to prevent aliasing of different frequencies. For example, speech signals generally have information up to 8kHz, so many speech signals are sampled at 16kHz. Music is more complex in that signals often span up to about 20kHz, so CD quality recordings are often sampled at 44.1kHz or higher. For this thesis, we use recordings sampled at 44.1kHz or lower.

2.3.2 Convolution

The discrete-time convolution operation takes two sequences $x[n]$ and $h[n]$ and outputs a third sequence $y[n] = x[n] * h[n]$:

$$y[n] = \sum_{k=-\infty}^{\infty} x[k]h[n-k] \quad (14)$$

Convolution is commutative, so $x[n] * h[n] = h[n] * x[n]$ holds true.

A linear, time-invariant (LTI) system is characterized by its impulse response $h[n]$, which allows us to determine samples $y[n]$ when $x[n]$ is subject to $h[n]$. For the purposes of this thesis, our underlying clean signal $x[n]$ might be subject to the conditions of an acoustic environment $h[n]$ and crowd noise $N[n]$:

$$y[n] = h[n] * x[n] + N[n] \quad (15)$$

In this scenario, our system would attempt to recover $h[n] * x[n]$ and possibly even $x[n]$ if the acoustic environment were deemed “noisy enough” due to echo and reverberation.

One of our proposed systems also incorporates convolutional neural networks (CNN) which use convolutions between frames of samples instead of simple linear combinations (discussed later).

2.3.3 Frequency Transforms

In some of our proposed systems, we use a frequency transformed version of the input signal as a preprocessing step to the system input. While no new information is gained from transforming the input, networks often respond better to determining the value of the magnitude of varying frequencies at a time slice instead of the individual time samples.

The frequency transform we use in this thesis is the discrete-time Fourier transform (DTFT). A sequence of N discrete-time samples is transformed into another sequence of N samples where each index then corresponds to a frequency bin. The DTFT $X[k]$ of a signal $x[n]$ is given by the following:

$$X[k] = \sum_{n=0}^{N-1} x[n] W_N^{kn} \quad (16)$$

where the twiddle factor W_N is given by $W_N = e^{-j(2\pi/N)}$. Then the reconstruction of $x[n]$ from $X[k]$ is given by:

$$x[n] = \frac{1}{N} \sum_{k=0}^{N-1} X[k] W_N^{-kn} \quad (17)$$

In this thesis, we also exploit the main duality between the time and frequency domain using the convolution theorem, which states that convolution in time is equivalent to multiplication in frequency and vice versa:

$$\mathcal{F}\{h[n] * x[n]\} = H[k]X[k] \quad (18)$$

$$\mathcal{F}^{-1}\{H[k] * X[k]\} = h[n]x[n] \quad (19)$$

This allows us to effectively treat our network as a non-linear filter that can denoise small time/frequency slices of our noisy signal, which can then be pieced back together using overlap-add resynthesis. We detail this in the next section.

2.3.4 Windowing and Perfect Reconstruction

To window a signal is to multiply a window function $w[n]$ by the frame, i.e. $w[n]x[n]$ over the frame length N . Because we are training a network to denoise small segments of a larger audio signal, we window the signal segments. This accommodates the finite-length requirement of the DTFT and helps to prevent spectral leakage. [6]

Also, to be able to properly reconstruct our signal, we use a window function and corresponding overlapping frame percentage to accomplish perfect reconstruction. The corresponding overlapping frame percentage is set such that the window sums to a constant for all time. For example, a rectangular window $w[n] = 1$ over an interval of length N has an overlap of 0% to sum to a constant 1 for all time. Another popular window is the Hanning window, defined over an interval N by the following:

$$w[n] = \frac{1}{2} \left(1 - \cos \left(\frac{2\pi n}{N-1} \right) \right) \quad (20)$$

For the Hann window, the perfect reconstruction overlap is a frame length of $N = 50\%$.

2.3.5 Window Size and Frequency v. Time Resolution Tradeoff

We must consider window size as a hyperparameter to our system. In general, shorter windows give rise to better time resolution at the cost of frequency resolution. On the other hand, longer windows give rise to better frequency resolution at the cost of time resolution. To illustrate, consider FIGURE.

2.3.6 Noise and Signal-to-Noise Ratio

Since we are trying to denoise audio signals, we must discuss how we measure noise. One of the most common measures of degradation of signal quality from additive noise is signal-to-noise ratio (SNR), defined as the ratio of signal variance to noise variance. [DSP] For the signal $y[n] = x[n] + N[n]$, where $x[n]$ is the signal of interest and $N[n]$ is the additive noise, the SNR is defined as

$$SNR = \frac{\sigma_x^2}{\sigma_n^2} \quad (21)$$

where σ^2 refers to the variance of the signal in question over some time interval. For the purposes of this thesis, we achieve desired a desired SNR for a simulation by scaling the noise to match the variance to the signal, then scaling the noise or the signal to achieve the desired SNR.

2.3.7 Magnitude and Phase Spectrum

3 Signal Model and Data

3.1 Network Input and Output

To simulate an audio denoising scheme, we define the following inputs and outputs. We take a known clean signal $x[n]$ which we subject to additive noise $N[n]$ using a specified SNR, resulting in the following noisy signal $y[n]$:

$$y[n] = x[n] + N[n] \quad (22)$$

To achieve a particular average SNR per simulation, we take the average signal energy for each minibatch of size B to determine a multiplicative scale factor k on the noise signal $N[n]$. For example, for additive white Gaussian noise (AWGN), we sample from the zero-mean, unit variance normal distribution (“randn” in Python) and determine our scale factor k as σ using the specified SNR in decibels:

$$\sigma_n^2 = \frac{1}{SNR_{lin}} \frac{1}{BN} \sum_{b=0}^{B-1} \sum_{n=0}^{N-1} x_b^2[n] \quad (23)$$

where SNR_{lin} is given by

$$SNR_{lin} = 10^{\frac{SNR_{db}}{10}} \quad (24)$$

In supervised scenarios, we allow the network to train with access to the ground truth $x[n]$. On the other hand, in semi-supervised scenarios, we only allow the network to train with access to a “soft label” indicating if the signal is (1) noise-only or (2) noise and possibly signal. [1] However, in both supervised and semi-supervised scenarios, our neural network input is one of the following:

1. Frames of $y[n]$
2. Frames of $\|Y[k]\|$
3. Magnitude spectrogram frames of $Y[k]$
4. Complex spectrogram frames of $Y[k]$

We choose the frame length L , time-domain window $w[n]$, and frame overlap percentage p as hyperparameters. Generally, we use 1024-sample frames at 16 kHz with a Hanning window with 50% overlap unless otherwise specified. In addition, for frequency frames, we use an FFT length the same length as our frame for a total of $L/2$ frequency bins. Note that our choice of frame length and sampling rate allows us to balance time and frequency resolution. With the given frame length and sampling rate, we achieve a frequency resolution of 15.625 Hz/bin by the following:

$$\frac{f_s/2 \text{ Hz}}{N/2 \text{ bins}} = \frac{f_s}{N} \quad (25)$$

$$= 15.625 \text{ Hz/bin} \quad (26)$$

Similary, our time resolution is given by

$$\frac{N}{f_s} = 64 \text{ msec} \quad (27)$$

Since we want to evaluate the level of denoising in the time domain, we recombine the network outputs with the noisy phase components of the spectrum if necessary to obtain an estimate $\hat{x}[n]$. We then compare $\hat{x}[n]$ to $x[n]$, in general using the mean squared error (MSE). For example, when our network outputs

frames of $\|\hat{X}[k]\|$, we take the inverse Fast Fourier transform (IFFT) using the noisy phase $\angle Y[k]$ and use overlap-add to recombine the frames:

$$x[n] = \mathcal{F}^{-1}\{\|\hat{X}[k]\|e^{j\angle Y[k]}\} \quad (28)$$

3.2 Signal and Noise Choices

Our choice of signals include the following:

1. Sine waves with multiple frequencies and random amplitudes and phases
2. Clean speech signals
3. Studio music recordings
4. Live concert recordings

Similarly, our choice of noise signals include the following:

1. Additive white Gaussian noise (AWGN)
2. Restaurant noise

As mentioned above, we can use the average energy per minibatch to specify a given SNR for an experiment. We take several combinations of clean and noise signals and compare across multiple SNRs.

3.3 Other Network Parameters

Since our networks involve one or more neural network layers, we show some results compared to choices of nonlinearity, number of layers (depth), and number of nodes in each layer (width). Generally, we use an identity at the

1350 network output and either the rectified linear unit (ReLU), a modified ReLU
1351
1352 (mReLU), leaky rectify, hyperbolic tangent (tanh), or an exponential linear
1353
1354 unit (elu).
1355
1356
1357
1358
1359
1360
1361
1362
1363
1364
1365
1366
1367
1368
1369
1370
1371
1372
1373
1374
1375
1376
1377
1378
1379
1380
1381
1382
1383
1384
1385
1386
1387
1388
1389
1390
1391
1392
1393
1394
1395
1396
1397
1398
1399
1400
1401
1402
1403

4 De-noising Architectures

In the following sections, we detail all considered shallow network architectures. Note that these network architectures can easily be extended to deep networks by adding corresponding encode and decode layers before and after the latent representation, respectively. These networks can be trained using the various inputs detailed in Chapter 3. However, for the purposes of presenting first results, we consider single FFT frames only to compare networks.

4.1 Supervised Autoencoder

We adopt the shallow supervised autoencoder from [2]. Used for supervised denoising, we adopt the relative network size as well as their modified nonlinear activation function. The network structure is a single hidden layer, dense neural network. In other words, we can represent our network output $\hat{X}_i[k]$ for various overlapping frames $i = 1, \dots, N$ by the following:

$$\hat{X}_i[k] = f_1(\mathbf{W}^{(1)}\mathbf{h}_i^{(0)} + \mathbf{b}^{(1)}) \quad (29)$$

$$\mathbf{h}_i^{(0)} = f_0(\mathbf{W}^{(0)}Y_i[k] + \mathbf{b}^{(0)}) \quad (30)$$

This network is trained to estimate the various layer weight matrices $\mathbf{W}^{(l)}$ and layer bias vectors $\mathbf{b}^{(l)}$.

Since we are estimating a magnitude spectrogram for values in the interval $[0, \infty)$, we use a nonlinear activation function whose support is on the same interval. A natural choice is the rectified linear unit (ReLU). However, as detailed in [2], the ReLU is subject to a 0-derivative for negative values. The modified ReLU used in [2], which we denote as mReLU, is given by the following:

$$f(x) = \begin{cases} x & \text{if } x \geq \epsilon \\ \frac{-\epsilon}{x-1-\epsilon} & \text{if } x < \epsilon \end{cases} \quad (31)$$

The choice of ϵ used in [2] is 10^{-5} . This modified ReLU allows for nodes to escape zero state since the derivative is always positive. An example plot of the nonlinearity is given in 2.

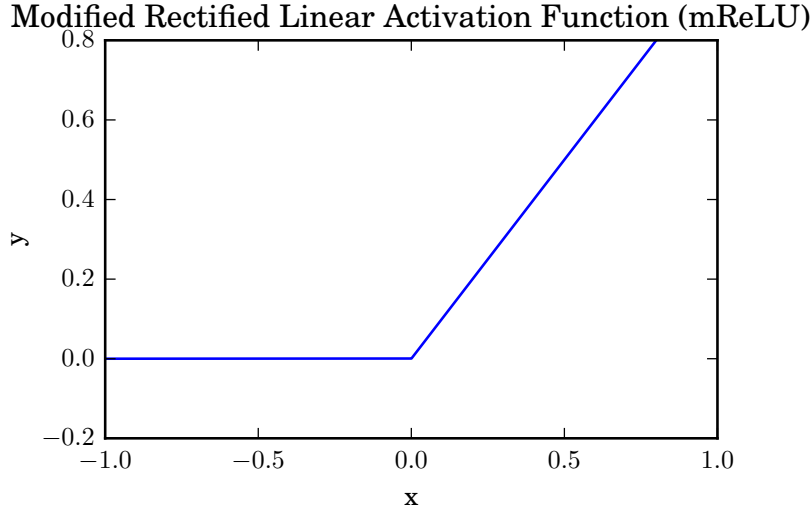


Figure 2: Modified Rectified Linear Unit Activation Function Plot

Since this network is supervised, we allow the training access to the original magnitude spectra $X[k]$. The loss function for training this network is defined as the mean squared error (MSE) between the network output and the clean spectra $X[k]$:

$$l(\mathbf{X}, \hat{\mathbf{X}}) = \|\mathbf{X} - \hat{\mathbf{X}}\|^2 \quad (32)$$

For our simulations, we also apply batch normalization at the input to help train more quickly and efficiently.

4.2 Partitioned Autoencoder

Adopted from [1], the partitioned autoencoder is a variation of a traditional autoencoder in which we do not know the noise corruption process or the underlying clean signals directly. This model more closely models a practical scenario. Since we don't have access to clean data, we rely instead on a "soft" label indicating whether we have a "noise-only" training example or a "noisy" training example which possibly has the desired signal present within it.

Depending on a number of factors, a traditional autoencoder can learn many different latent representations which ultimately learn to encode and decode the underlying clean signal. A partitioned autoencoder seeks to use regularization during training to give explicit meaning to the latent variables in the network. If we can identify noise-only components in our training data, we can potentially train the network to put noise-only information into one part of the latent space. Then, the rest of the latent variables should correspond to signal-only if a sufficient representation of the noise is learned. At inference time, we can then zero out the noise-only latent variables to accomplish denoising.

In [1], they use the following loss function to accomplish effective partitioning:

$$l(\mathbf{Y}, y) = \|\mathbf{Y} - \hat{\mathbf{X}}\|^2 + \frac{\lambda y}{\mathbf{C}} \|\mathbf{C} \odot f(\mathbf{Y})\|^2 \quad (33)$$

where $\hat{\mathbf{X}} = g(f(\mathbf{Y}))$, the latent variables are given by $f(\mathbf{Y})$, \mathbf{C} is a masking matrix dependent on the minibatch and latent sizes taking on the value 1 for signal latents and 0 for noise or background latents. y corresponds to the aforementioned soft label which has value 0 for a signal-plus-noise example and 1 for a noise-only example. λ is a regularization coefficient which is set to

a higher value than normally used for regularization to enforce zeroing out of signal-based latents for noise-only examples.

In other words, when we train the network, we use minibatches with fixed ordering corresponding to the same proportion of signal-plus-noise examples and noise-only examples such that \mathbf{C} does not change on each training iteration. An example \mathbf{C} is given in Figure 3. For signal-plus-noise examples, the regularization term is 0, and the network seeks to reconstruct the noisy example. However, for noise-only examples, the network tries to put all of the latent energy into the pre-determined noise-only latent variables. In [1], they balance this by choosing 25% of minibatches to be noise-only as well as 25% of latent variables to be noise-only.

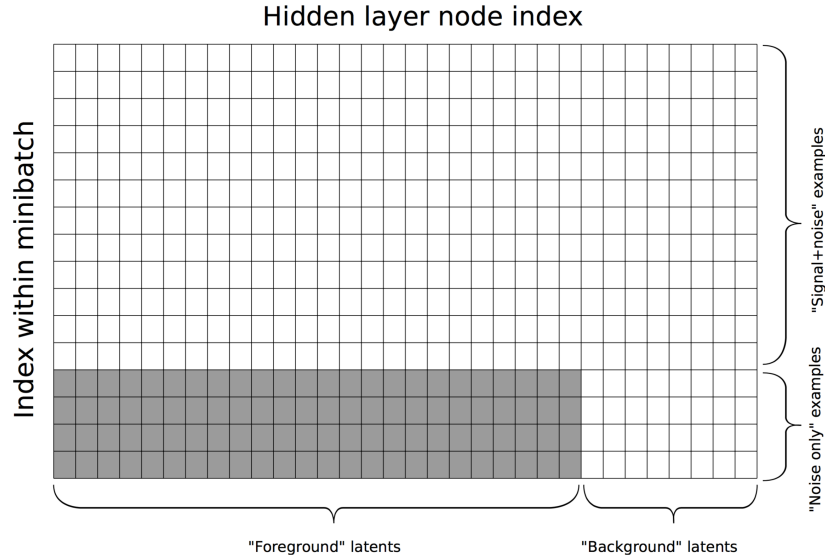


Figure 3: Example Partitioned Masking Matrix. [1] The gray area corresponds to signal (foreground) latents for noise-only examples. We want to penalize the network for any nonzero energy in the signal latents when there are noise-only examples.

Note that it is okay for noise-only examples to be mislabeled as signal-plus-noise, but the opposite would cause the signal to be misrepresented as noise.

Therefore, the soft labeling of examples should be cautious on the side of labeling as noise-only.

In [1], they use spectrogram frames as input. Their partitioned autoencoder is constructed as a shallow two-dimensional convolutional autoencoder with input normalization to zero-mean and unit-variance, maxpooling along the time index, and a ReLU nonlinearity before the latent layer. Their convolutional layer is constructed such that the frequency space is fully connected, and the convolution happens in time. The results of their autoencoder are presented in the frequency domain only, so we seek to adapt the partitioning concept to also recover cleaner time-domain audio.

Therefore, we use the same loss function as defined in Equation 33, but we use single magnitude spectrum frames and compare results on the mean squared error in the time-domain rather than in the frequency domain as their results presented. We also used the modified ReLU as presented from [2].

4.2.1 Phase Reconstruction

By extension, we combine the estimated magnitude spectra at the output with the original noisy phase. We can then recover a time-domain estimate of our desired signal using overlap-add resynthesis.

Other experiments we tried involved trying to explicitly or implicitly estimate the clean phase. One such explicit experiment involved training a parallel partitioned autoencoder with modified nonlinearities that tried to learn a clean phase representation. However, this ended up with a worse MSE and distorted the signal than using the original noisy phase. An implicit phase estimation example involved training the network using two channels as feature maps, where the real part of the frequency spectrum made up one feature map and

the imaginary part of the frequency spectrum made up the other. This also resulted in worse reconstructed signals than the case where we estimate the magnitude spectrum and combine with the noisy phase. Sample code is provided in the appendix.

4.3 Curro Autoencoder

We present here the Curro Partitioned Autoencoder, a novel partitioned neural network architecture. Similar to [1], we exploit the latent space structure to put noise and signal energy into different latent variables. A basic overview of the network is detailed in Figure [FIG].

In the shallow case, we have an input layer, a fully connected hidden layer, and then a split in the latent space. We split the network such that half of the latent variables correspond to signal and the other half correspond to noise, and then the outputs from both network partitions are summed. For the shallow case, we use one fully connected layer followed by an output layer of the same size. The parallel networks are the same size and share the same parameters \mathbf{W} and \mathbf{b} . Unlike in [1], we constrain the problem to 50% of latent variables for signal content and 50% for noise content. While there may be drawbacks to such a restriction, the benefit here is that we do not have to choose that ratio as a hyperparameter.

More formally,

$$\hat{Y}_i[k] = \hat{X}_i[k] + \hat{N}_i[k] \quad (34)$$

where

1728
1729
1730
1731
1732
1733
1734
1735
1736
1737
1738
1739
1740
1741
1742
1743
1744
1745
1746
1747
1748
1749
1750
1751
1752
1753
1754
1755
1756
1757
1758
1759
1760
1761
1762
1763
1764
1765
1766
1767
1768
1769
1770
1771
1772
1773
1774
1775
1776
1777
1778
1779
1780
1781

$$\hat{X}_i[k] = \mathbf{W}^{(3)} f(\mathbf{W}^{(2)} \mathbf{z}_{1/2} + \mathbf{b}^{(2)}) + \mathbf{b}^{(3)} \quad (35)$$

5 Results

5.1 Supervised Autoencoder

For the following results, we show

5.1.1 Batch Normalized Input

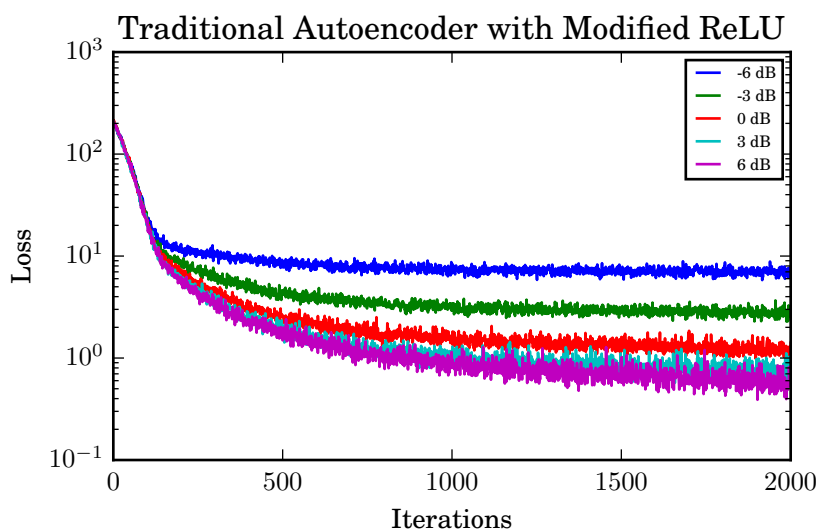


Figure 4: Loss at various SNRs for Supervised Single-Layer Autoencoder with Batch Normalization at the Input

5.1.2 Non-Batch Normalized Input

5.2 Partitioned Autoencoder

5.3 Partitioned Curro Autoencoder

5.4 Comparison of Loss Convergence

5.5 Comparison of Mean Squared Error Convergence

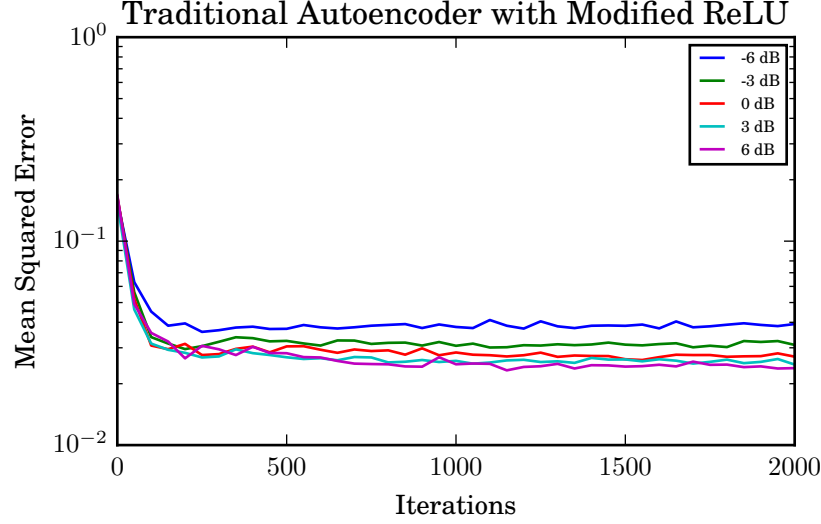


Figure 5: MSE at various SNRs for Supervised Single-Layer Autoencoder with Batch Normalization at the Input

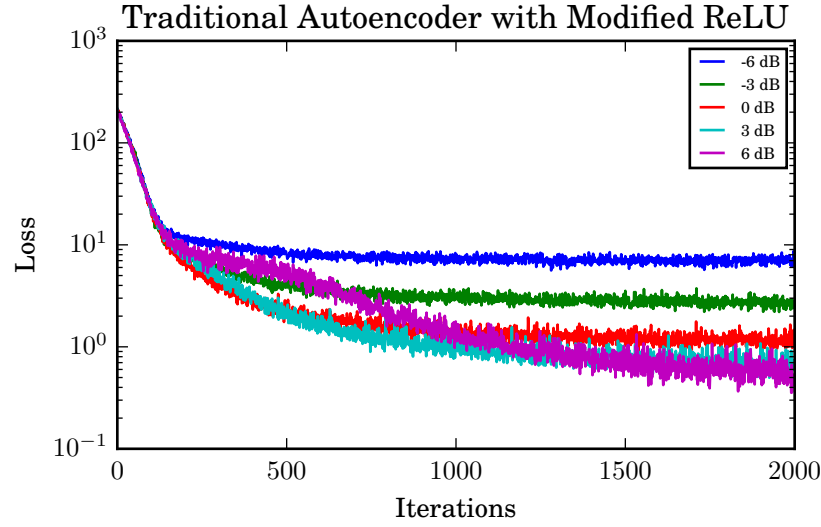


Figure 6: Loss at various SNRs for Supervised Single-Layer Autoencoder without Batch Normalization at the Input

6 Conclusions and Future Work

6.1 Conclusions

While more work is needed, deep partitioned neural network architectures using time and frequency data seem promising in long-term solutions for denoising speech and music signals.

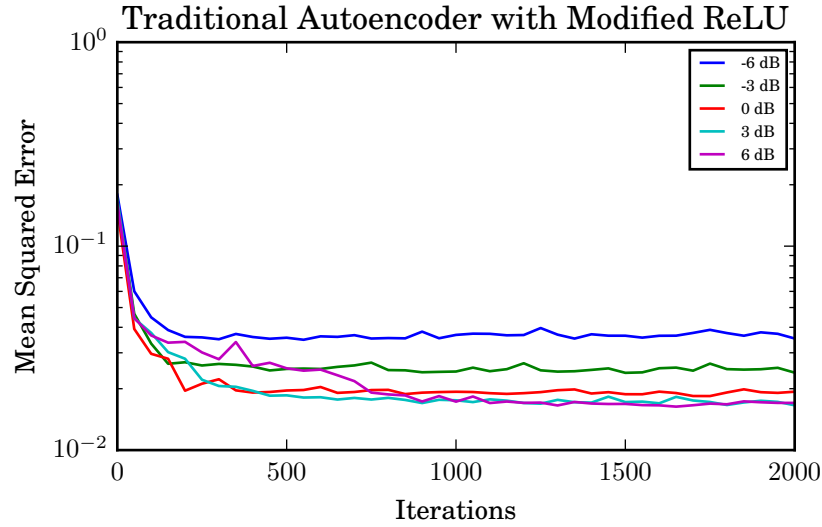


Figure 7: MSE at various SNRs for Supervised Single-Layer Autoencoder with Batch Normalization at the Input

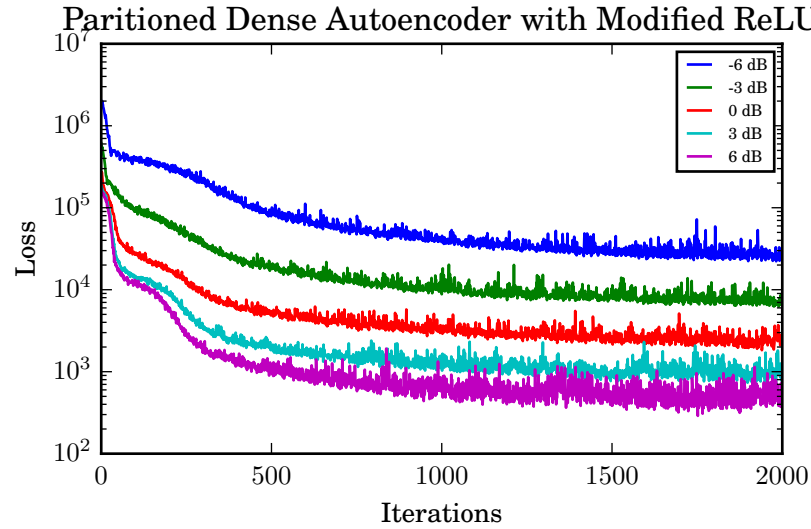


Figure 8: Loss at various SNRs for Single-Layer Partitioned Autoencoder [1]

6.2 Future Work

6.2.1 Models

Make network deeper. Consider gradual partitioning instead of hard.

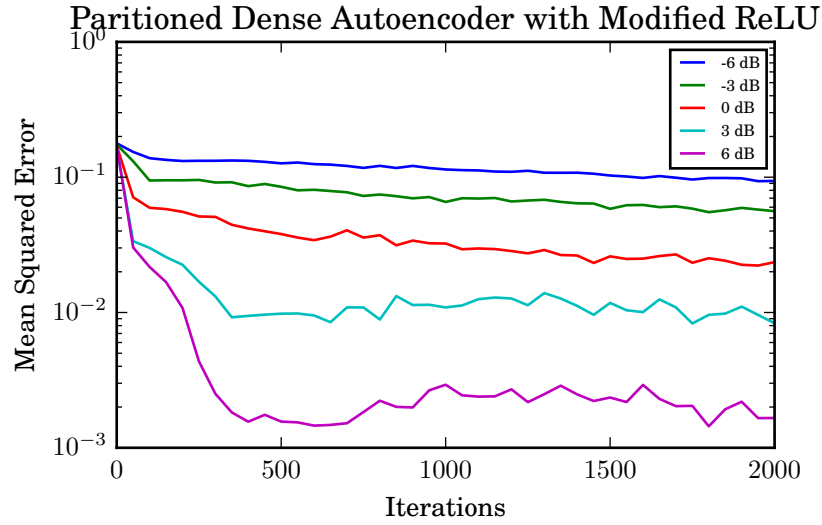


Figure 9: MSE at various SNRs for Single-Layer Partitioned Autoencoder [1]

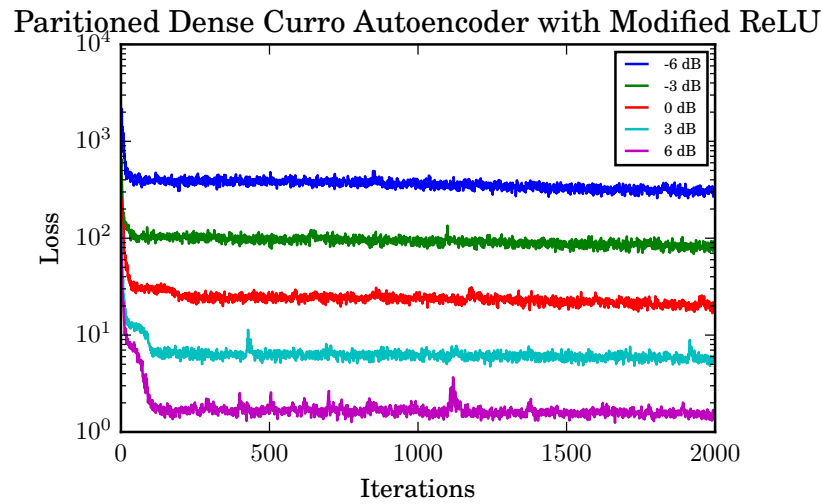


Figure 10: Loss at various SNRs for Single-Layer Curro Autoencoder

6.2.2 Data

Get more data. Consider different noise levels and types of signals.

1998
1999
2000
2001
2002
2003
2004
2005
2006
2007
2008
2009
2010
2011
2012
2013
2014
2015
2016
2017
2018
2019
2020
2021
2022
2023
2024
2025
2026
2027
2028
2029
2030
2031
2032
2033
2034
2035
2036
2037
2038
2039
2040
2041
2042
2043
2044
2045
2046
2047
2048
2049
2050
2051

Partitioned Dense Curro Autoencoder with Modified ReLU

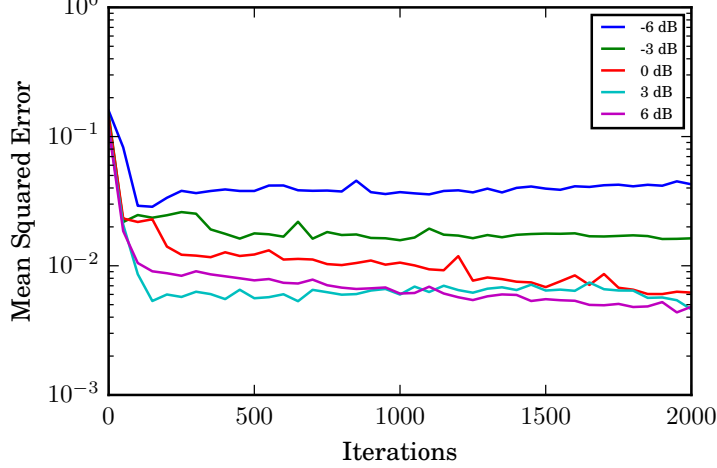


Figure 11: MSE at various SNRs for Single-Layer Curro Autoencoder

Comparison of loss of various networks at -6 dB

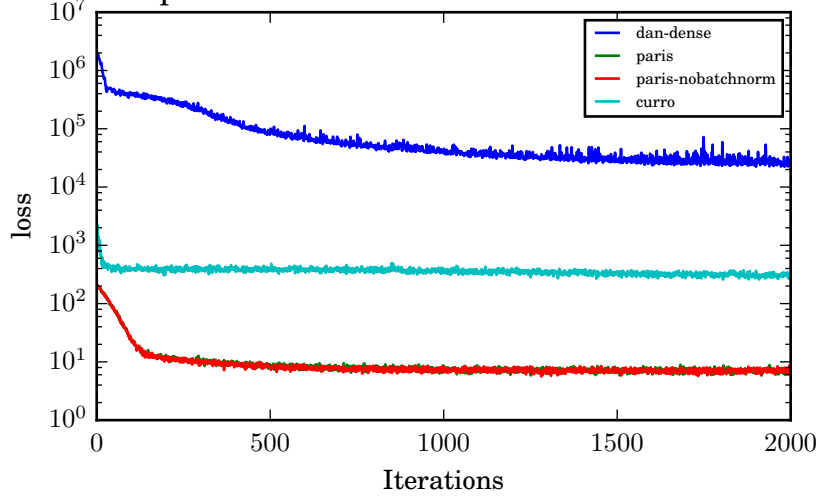


Figure 12: Loss Comparison of Various Networks at -6 dB

References

- [1] D. Stowell and R. E. Turner, "Denoising without access to clean data using a partitioned autoencoder," *CoRR*, vol. abs/1509.05982, 2015. [Online]. Available: <http://arxiv.org/abs/1509.05982>
- [2] D. Liu, P. Smaragdis, and M. Kim, "Experiments on deep learning for speech denoising." in *INTERSPEECH*, 2014, pp. 2685–2689.
- [3] C. M. Bishop, *Pattern recognition and machine learning*. springer, 2006.

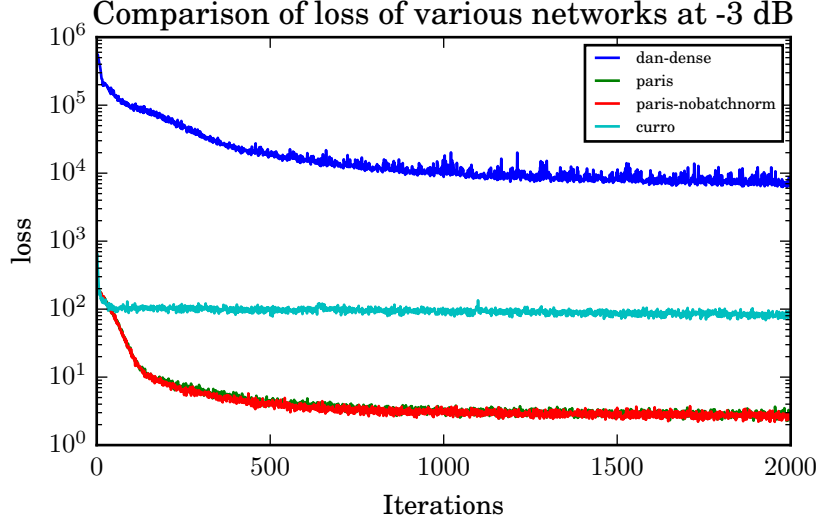


Figure 13: Loss Comparison of Various Networks at -3 dB

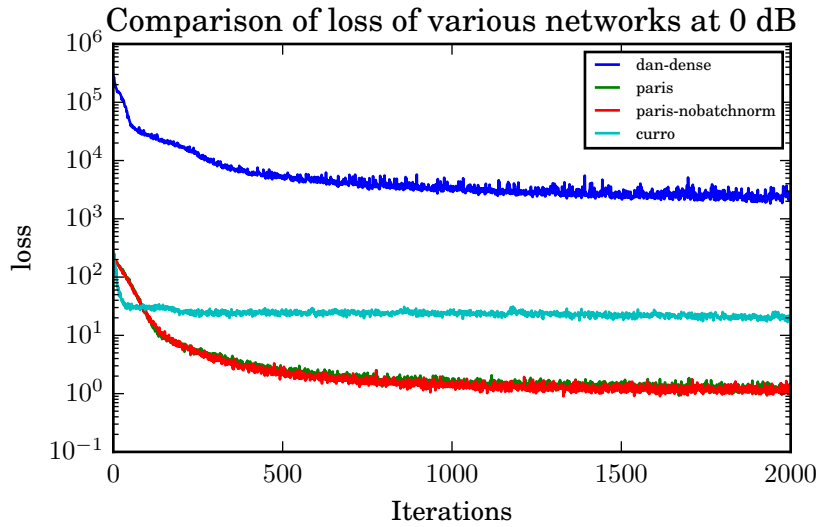


Figure 14: Loss Comparison of Various Networks at 0 dB

- [4] X. Glorot, A. Bordes, and Y. Bengio, "Deep sparse rectifier neural networks." in *Aistats*, vol. 15, no. 106, 2011, p. 275.
- [5] D. R. Wilson and T. R. Martinez, "The general inefficiency of batch training for gradient descent learning," *Neural Networks*, vol. 16, no. 10, pp. 1429–1451, 2003.
- [6] V. O. Alan, W. S. Ronald, and R. John, "Discrete-time signal processing," *New Jersey, Printice Hall Inc*, 1989.

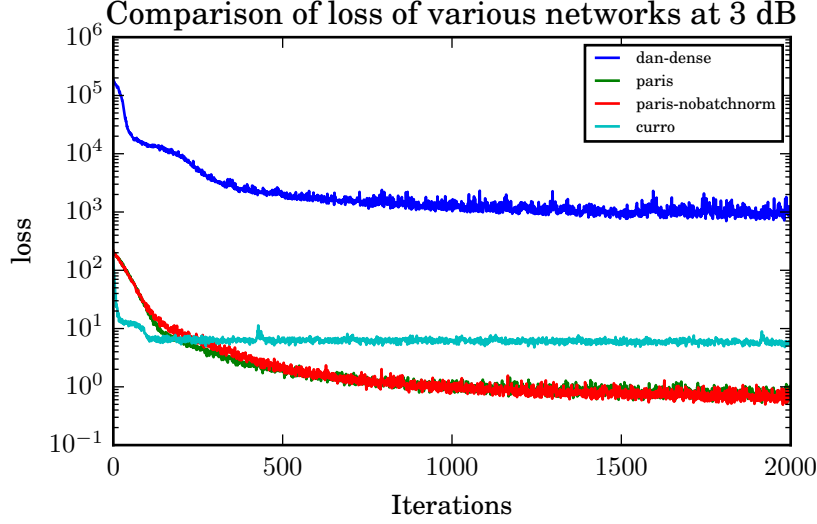


Figure 15: Loss Comparison of Various Networks at 3 dB

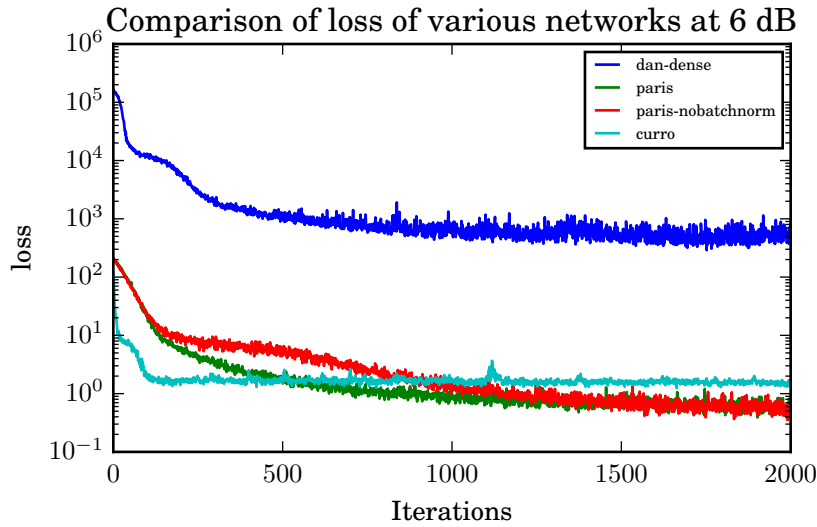


Figure 16: Loss Comparison of Various Networks at 6 dB

- [7] P. Baldi and Z. Lu, "Complex-valued autoencoders," *Neural Networks*, vol. 33, pp. 136–147, 2012.
- [8] Y. Xu, J. Du, L.-R. Dai, and C.-H. Lee, "An experimental study on speech enhancement based on deep neural networks," *IEEE Signal Processing Letters*, vol. 21, no. 1, pp. 65–68, 2014.
- [9] P. Vincent, H. Larochelle, I. Lajoie, Y. Bengio, and P.-A. Manzagol, "Stacked denoising autoencoders: Learning useful representations in a

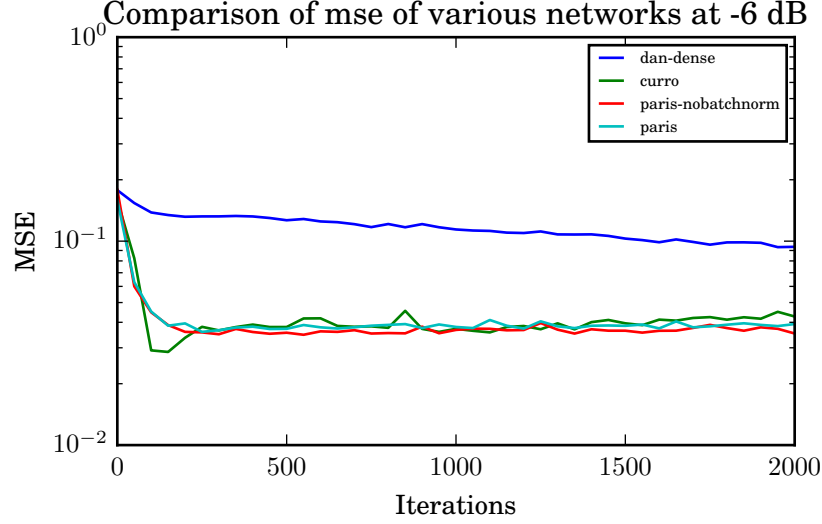


Figure 17: MSE Comparison of Networks at -6 dB

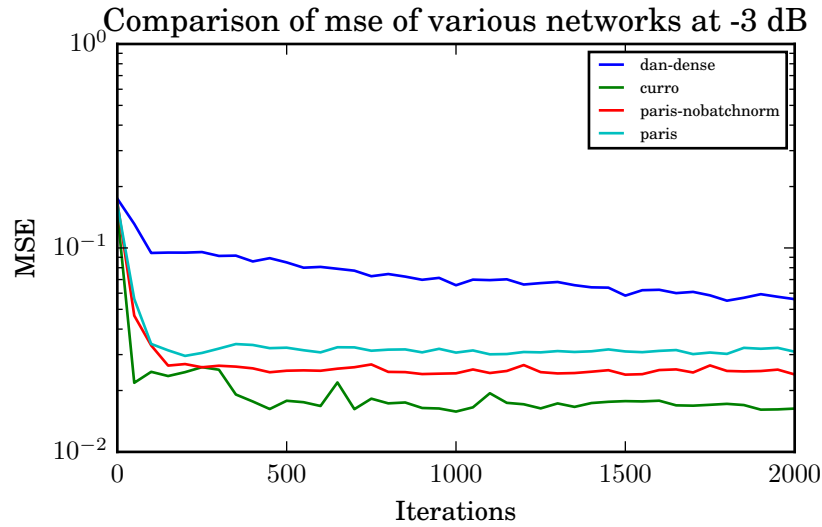


Figure 18: MSE Comparison of Networks at -3 dB

deep network with a local denoising criterion,” *Journal of Machine Learning Research*, vol. 11, no. Dec, pp. 3371–3408, 2010.

- [10] T. Ishii, H. Komiyama, T. Shinozaki, Y. Horiuchi, and S. Kuroiwa, “Reverberant speech recognition based on denoising autoencoder.” in *INTER-SPEECH*, 2013, pp. 3512–3516.
- [11] B. Gold, N. Morgan, and D. Ellis, “Speech and audio signal processing: processing and perception of speech and music,” 2011.

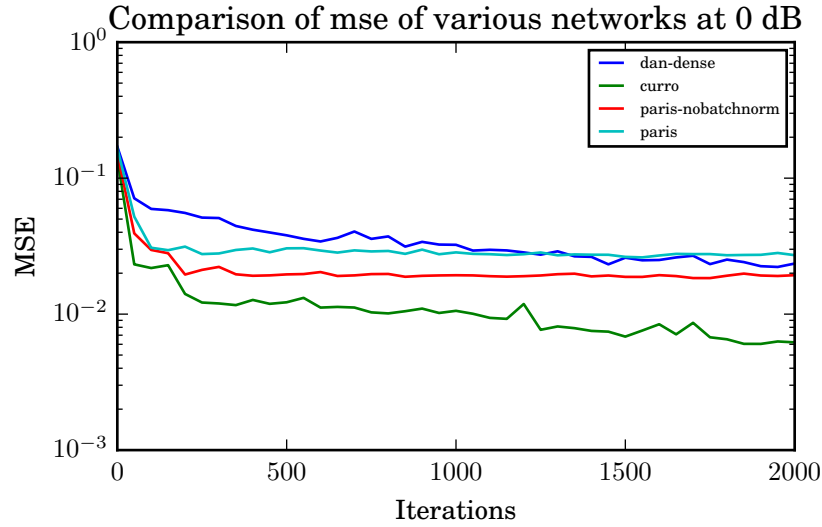


Figure 19: MSE Comparison of Networks at 0 dB

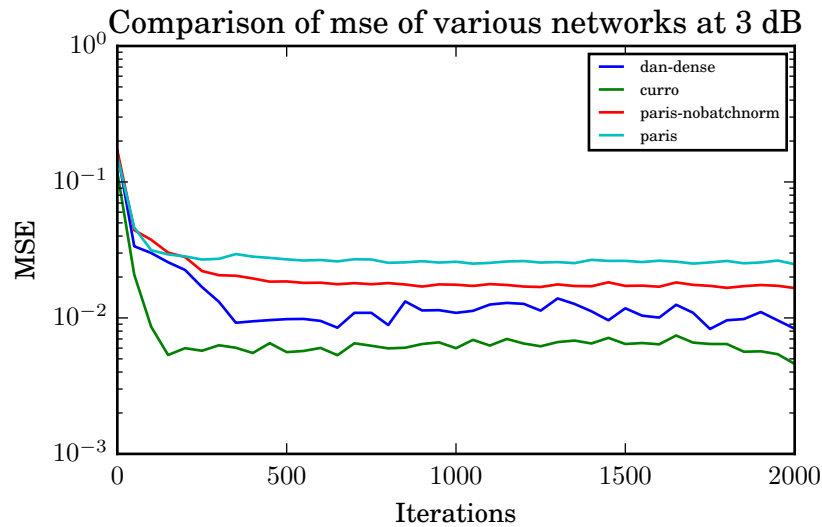


Figure 20: MSE Comparison of Networks at 3 dB

- [12] M. Kayser and V. Zhong, “Denoising convolutional autoencoders for noisy speech recognition.”
- [13] U. Zölzer, *Digital audio signal processing*. John Wiley & Sons, 2008.
- [14] G. E. Hinton and R. R. Salakhutdinov, “Reducing the dimensionality of data with neural networks,” *Science*, vol. 313, no. 5786, pp. 504–507, 2006.
- [15] A. Rad and T. Virtanen, “Phase spectrum prediction of audio signals,”

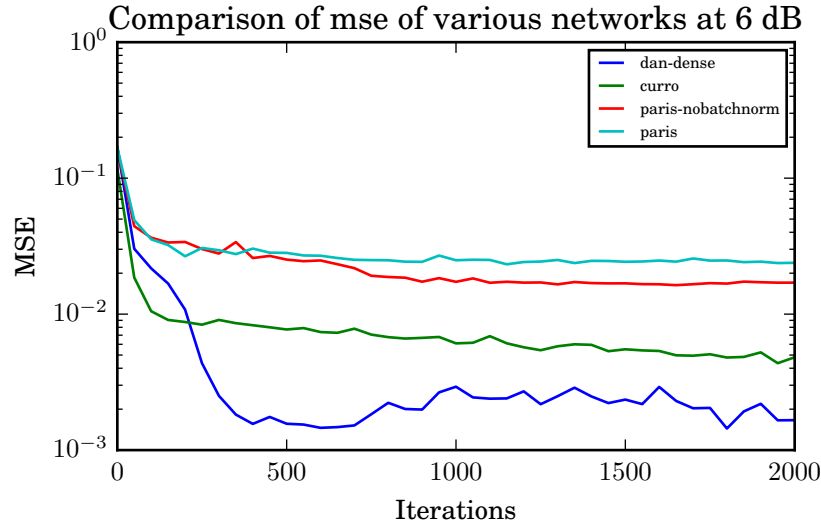


Figure 21: MSE Comparison of Networks at 6 dB

in *International Symposium on Communications Control and Signal Processing (ISCCSP)*, 2012, pp. 1–5.

- [16] Theano Development Team, “Theano: A Python framework for fast computation of mathematical expressions,” *arXiv e-prints*, vol. abs/1605.02688, May 2016. [Online]. Available: <http://arxiv.org/abs/1605.02688>
- [17] S. Dieleman, J. Schlüter, C. Raffel, E. Olson, S. K. Sønderby, D. Nouri, D. Maturana, M. Thoma, E. Battenberg, J. Kelly, J. D. Fauw, M. Heilman, diogo149, B. McFee, H. Weideman, takacsg84, peterderivaz, Jon, instagibbs, D. K. Rasul, CongLiu, Britefury, and J. Degraeve, “Lasagne: First release.” Aug. 2015. [Online]. Available: <http://dx.doi.org/10.5281/zenodo.27878>
- [18] S. Ioffe and C. Szegedy, “Batch normalization: Accelerating deep network training by reducing internal covariate shift,” *arXiv preprint arXiv:1502.03167*, 2015.
- [19] P. Vincent, H. Larochelle, Y. Bengio, and P.-A. Manzagol, “Extracting and composing robust features with denoising autoencoders,” in *Proceedings of the Twenty-fifth International Conference on Machine Learning (ICML’08)*, W. W. Cohen, A. McCallum, and S. T. Roweis, Eds. ACM, 2008, pp. 1096–1103.

2322 [20] W. W. Cohen, A. McCallum, and S. T. Roweis, Eds., *Proceedings of the*
2323 *Twenty-fifth International Conference on Machine Learning (ICML'08)*.
2324 ACM, 2008.
2325
2326
2327 [21] (2010) Denoising autoencoders (da). [Online]. Available:
2328 <http://deeplearning.net/dA.html>
2329
2330 [22] S. Sonoda and N. Murata, “Decoding stacked denoising au-
2331 toencoders,” *CoRR*, vol. abs/1605.02832, 2016. [Online]. Available:
2332 <http://arxiv.org/abs/1605.02832>
2333
2334
2335
2336
2337
2338
2339
2340
2341
2342
2343
2344
2345
2346
2347
2348
2349
2350
2351
2352
2353
2354
2355
2356
2357
2358
2359
2360
2361
2362
2363
2364
2365
2366
2367
2368
2369
2370
2371
2372
2373
2374
2375